Journal Pre-proof

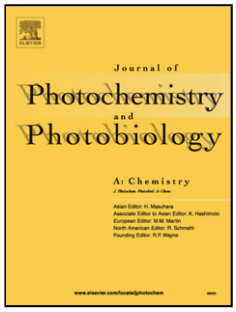

Novel Symmetric Schiff-Base Benzobisthiazole-Salicylidene Derivative with Fluorescence Turn-on Behavior for Detecting Pb^{2+} Ions

Marjan Rahimi, Abbas Amini, Hossein Behmadi

PII: S1010-6030(19)31539-4

DOI: https://doi.org/10.1016/j.jphotochem.2019.112190

Reference: JPC 112190

To appear in: *Journal of Photochemistry & Photobiology, A: Chemistry*

Received Date: 5 September 2019

Revised Date: 19 October 2019

Accepted Date: 21 October 2019

Please cite this article as: Rahimi M, Amini A, Behmadi H, Novel Symmetric Schiff-Base Benzobisthiazole-Salicylidene Derivative with Fluorescence Turn-on Behavior for Detecting Pb^{2+} Ions, *Journal of Photochemistry and amp; Photobiology, A: Chemistry* (2019), doi: https://doi.org/10.1016/j.jphotochem.2019.112190

This is a PDF file of an article that has undergone enhancements after acceptance, such as the addition of a cover page and metadata, and formatting for readability, but it is not yet the definitive version of record. This version will undergo additional copyediting, typesetting and review before it is published in its final form, but we are providing this version to give early visibility of the article. Please note that, during the production process, errors may be discovered which could affect the content, and all legal disclaimers that apply to the journal pertain.

© 2019 Published by Elsevier.

Journal Pre-proof

Novel Symmetric Schiff-Base Benzobisthiazole-Salicylidene Derivative with Fluorescence Turn-on Behavior for Detecting Pb^{2+} Ions

Marjan Rahimi[a], Abbas Amini[b,*], Hossein Behmadi[a]

[a]Department of Chemistry, Faculty of Science, Islamic Azad University, Mashhad Branch, P.O. Box: 91735-413, Mashhad, Iran

[b]Centre for Infrastructure Engineering, Western Sydney University, Penrith, NSW 2751, Australia

[*]Corresponding Author.

A. Amini: *E-mail*: a.amini@westernsydney.edu.au, Fax: +61-247360106, Tel.: +61-402850916

Graphical abstract

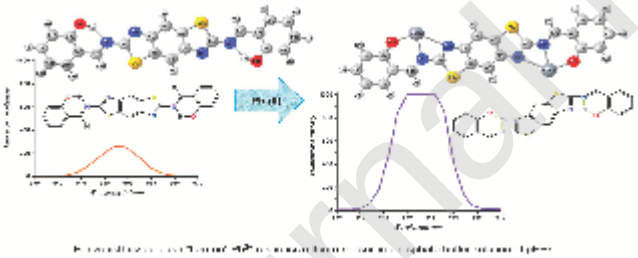

Highlights:

- Novel benzobisthiazole-salicylidene-base chemo-sensor showed large Stokes shift
- The ligand had enhanced emission in solution and solid-state due to aggregation
- Probe had fast turn-on Pb^{2+} ion detection in aqueous medium at physiological pH
- Detection limit and binding constants were 2.23×10^{-6} M and 0.41×10^{5} M^{-1}
- Computational studies confirmed the experimental sensory behavior of new ligand

Journal Pre-proof

Abstract

A novel ligand, N^2,N^6-bis(2-salicylidene)benzobisthiazole (BSBBT), was designed and synthesized with an excellent yield through a facile one-step condensation eco-reaction for fluorescent detection of Pb^{2+} ions. BSBBT was well-characterized through FT-IR, ^{1}H NMR, ^{13}C NMR, XRD for inclusive study of photo-physical behaviors. From the value of aggregation induced enhanced emission (AIEE) and excited-state intramolecular proton transfer (ESIPT) properties with a large Stocks shift (160 nm), BSBBT was characterized highly emissive in DMSO/H_2O (30:70, v/v) solution as well as in solid state. BSBBT showed a strong fast response and highly selective and sensitive "turn-on" fluorescent sensing behavior for detecting Pb^{2+} ions in phosphate buffer solution (PBS) without any interference from other metal cations at the physiological pH (~7). The calculated binding constant and detection limit were 0.41×10^5 M^{-1} and 2.23×10^{-6} M, respectively. Density Functional Theory calculation confirmed the formation of stable BSBBT-Pb^{2+} complex with a lower energy gap compared to BSBBT. BSBBT is the first high-efficient luminescent benzobisthiazole-base fluorescent sensor reported so far for detecting Pb^{2+} ions in PBS at the physiological pH range.

***Keywords*:** Fluorescent sensor, Benzobisthiazole-Salicylidene, tridentate ligand, Pb^{2+}, Schiff-base derivative

1. Introduction

Lead (Pb) with various usage in industries, including batteries, wires, paints, computers etc., is considered as the third most abundant toxic heavy metal circulating in soil and water resources [1]. Little intake of Lead can lead to permanent or serious damage to brain [2], immune system [3], liver and kidney [4], blood cells and memory [5]. As per its deadly role in ecology, biology and human health, the development of highly selective and sensitive sensors for easy, accurate and rapid tracing of Pb^{2+} ions is necessitated.

Journal Pre-proof

Various lab-on-the-chip chemo-sensors have been proposed for detecting Pb^{2+} ions on the basis of absorption and fluorescence spectroscopy through binding moieties and other components, such as peptide [6], protein [7], DNAzyme [8], polymer [9], carbon quantum dots [10], and supramolecular complexes of Bis(O_2S_2 macrocycle) [11]. These setups have serious drawbacks, including sophisticated instruments, complex data analysis, delayed response time, and significant interferences received from other transition metal ions. Among the probes, the fluorescence-base ones are very encouraging for detecting Pb^{2+}, as per their operational simplicity and reliability, high selectivity and sensitivity, and with the capability of being monitored by naked eyes.

Chromophore benzobisthiazole (BBTz or trans-BBTz) compounds are promising structures for photo-transistor equipment [12], photo-voltaic [13] and solar cells [14]. BBTz has delocalized π-expanded structure with over three fused conjugated aromatic rings made of a symmetric molecule. With high fluorescence property, thermal stability and electron affinity, BBTz is suitable for engineered chromophores which need two-photon absorption in the near-IR region [15], as well as hetero-aromatic systems which require diagnostic agents for 3D fluorescence imaging [16]. Sulfur atom is less electronegative than the oxygen atom with similar electronegativity to carbon atom. In BBTz, the electron density is shared more equally between sulfur and carbon, and thus the π-orbitals would be more delocalized. Empty *d* orbitals of the sulfur atom can contribute in the molecular π-orbitals, and that decrease the energy of π-π* transition [17]. Although BBTz molecules (with three conjugated heterocyclic rings) have been rarely reported in literature [18], many fluorescence probes containing benzothiazole (BTz) moieties (with two conjugated aromatic rings) have been used for detecting various bioactive analytes such as anions and cations (Table 1).

Most of sensitive fluorescent chemo-sensors for detecting Pb^{2+} are restricted to organic or a mixture of organic/aqueous solvents [19] due to their poor water solubility, hence, they cannot be used for biological media. So, designing a highly selective and sensitive probe for monitoring trace amount of Pb^{2+} in pure aqueous systems seems to be very challenging. To address this problem, we introduce and synthesize a novel Schiff-base chemo-sensor fluorescent probe, BSBBT, through a facile one-step and low-cost

Journal Pre-proof

condensation reaction. We take the advantage from two fluorophores, trans-BBTz and salicylaldehyde moieties, to construct a "turn-on" Pb^{2+} responsive fluoro-sensor in PBS. BSBBT structure acts on the basis of excited-state intramolecular proton transfer (ESIPT), originated from the keto and enol tautomers of salicylaldehyde moiety. Tautomerization-base fluorescent sensors are encouraging because of their dual fluorescence intensity changes at the near infrared zone (700–900 nm) and large Stokes shift. Stokes shift ($\Delta\lambda$) is the difference in the wavelength of maxima band of absorption and fluorescence emission spectra of similar electronic transition. In biological contexts, these sensors can act efficiently through prohibiting photo-damage caused by the self-absorbance and strong interference derived from short wavelength emission [20]. ESIPT molecules are useful building block materials for photonic devices, potentially suitable for white-light emission [21].

After synthesizing the BSBBT compound, the structural-induced photo-physical properties of BSBBT both in solution and solid state, pH-dependency, ESIPT properties, selectivity and sensitivity toward Pb^{2+} were thoroughly investigated. The Density Functional Theory (DFT) calculations were carried out to verify the electronic structure and geometry of new ligand, BSBBT. As far as we know, BSBBT is the first high-efficient luminescent BBTz-base fluorescent sensor reported so far for detecting Pb^{2+} ions in PBS at the physiological pH range. These significances indicate the potential applicability of BSBBT molecule for physiological and environmental purposes.

Table 1. Recent BTz moieties-base fluoro-sensor probes to detect various cations and anions in different solutions.

Solvent mixture (v/v)	**Ion detection**	**Merits; Drawbacks**	**DL[1] (M)**	**K_b[2] (M^{-1})**	**Ref.**
THF[3]/H_2O (1:1)	Hg^{2+}	Turn-on sensor, simple synthesis; Using toxic solvent, pH=8.5	1.59×10^{-8}	-	[22]
DMSO[4]/H_2O (2:98)	Cu^{2+} Hg^{2+}	Turn-on sensor for Hg^{2+}, pH=7.4[5], dual-target detection; Multi-step synthesis, turn-off sensor for Cu^{2+}, using toxic solvent	7.6×10^{-9}	$7.78\ 10^{4}$	[23]
THF/HEPES[6] (4:6)	Hg^{2+} Ag^{2+}	Turn-on sensor, pH=7.4, dual-target detection; Using toxic solvent, complex synthesis	0.27×10^{-6} 0.45×10^{-6}	4.04×10^{4} 1.22×10^{4}	[24]
DMF[7]/H_2O (96:4)	Al^{3+} Cr^{3+} Zn^{2+} F-	Multi-target detection, pH=7; Using high quantity of toxic solvent, multi-step synthesis	27×10^{-9} 25×10^{-9} 33×10^{-9} 67×10^{-9}	4.85×10^{6} 1.99×10^{7} 3.09×10^{7} 1.23×10^{5}	[25]

Journal Pre-proof

DMSO-PBS (3:1)	Pd^{2+}	Turn-on sensor, fluorescence signal in near-infrared pH=7.4; Using high quantity of toxic solvent, delayed response time, multi-step synthesis	48×10^{-9}	-	[26]
THF/H_2O (1:9)	Al^{3+}	Turn-on sensor, pH=7.4; Using toxic solvent, multi-step synthesis	2.2×10^{-6}	-	[27]
Methanol/H_2O (7:3)	Al^{3+} Zn^{2+} Cd^{2+}	Multi-target detection, pH=7.4; Using high quantity of toxic solvent	0.1×10^{-6}	-	[28]
Acetonitrile/ H_2O (5:5)	Cu^{2+}	Turn-on sensor, large Stokes shift; Using toxic solvent	3.2×10^{-9}	-	[29]
DMSO/H_2O (9:1)	Cysteine	Turn-on sensor; Using high quantity of toxic solvent	0.32×10^{-6}	-	[30]
DMF/H_2O (9:1)	Zn^{2+} Cd^{2+}	Dual-target detection, turn-on sensor; Using high quantity of toxic solvent	0.36×10^{-7} 1.16×10^{-6}	-	[31]
Buffer solution	Zn^{2+} PPi	pH=7.4, dual-target detection, turn-on sensor; Complex synthesis	7×10^{-9}	4.53×10^{4}	[32]
Ethanol-HEPES (65:35)	Zn^{2+}	Turn-on sensor, pH=7.2; Multi-step synthesis, interference from other cations	2.58×10^{-7}	4.04×10^{4}	[33]
Acetonitrile/ H_2O (9:1)		pH=7.4; Using high quantity of toxic solvent, multi-step synthesis	3.48×10^{-7}	2.40×10^{6}	[34]
Methanol/H_2O (1:1)		Turn-on sensor, simple synthesis; Using toxic solvent	6.7×10^{-8} 3.6×10^{-7}	4.9×10^{4} 2.1×10^{4}	[35]
DMSO/H_2O (3:2)		pH=7; Using high quantity of toxic solvent, multi-step synthesis	35×10^{-9}	9.95×10^{5}	[36]
THF/H_2O (1:9)	Picric acid	Aqueous solution; Using toxic solvent, multi-step synthesis	-	-	[37]
EtOH/PBS buffer (3:7)	Au^{3+}	pH=7.4, dual fluorescence response; Costly	9×10^{-9}	-	[38]
Acetonitrile, DMSO, Ethanol/H_2O (3:1)	F^-	Ratiometric sensor; Turn-off sensor, using high quantity of toxic solvent	73×10^{-9} 138×10^{-9}	-	[39]
DMSO/HEPES (4:6)	Cu^{2+} PO_4^{3-}	Dual-target detection, pH=7.35; Using toxic solvent, multi-step synthesis	1.018×10^{-8} 1.52×10^{-7}	-	[40]
100% aqueous solution	Cu^{2+} S^{2-}	Dual-target detection, pH=7.4, 100% aqueous solution, large Stokes shift; Turn-off sensor, multi-step synthesis	63×10^{-9}	-	[41]
DMF/H_2O (1:9)	CN^-	Turn-on sensor, pH=7.4; Using toxic solvent	0.15×10^{-6}	-	[42]
Aqueous buffer solution	Thiophenol	Turn-on sensor, large Stokes shift, pH=7.4; Complex synthesis	2.9×10^{-9}	-	[43]
100% aqueous buffer solution	Pb^{2+}	Turn-on sensor, fast response, large Stokes shift, pH=7.4, using 100% aqueous solution, one-step synthesis, high yield product, AIE-active molecule, no interference from other metal ions	2.23×10^{-6}	0.41×10^{5}	**This work**

[1] DL: Detection Limit
[2] K_b: Binding Constant
[3] THF: Tetrahydrofuran
[4] DMSO: dimethyl sulfoxide
[5] pH=7.4; Physiological pH
[6] HEPES: (4-(2-hydroxyethyl)-1-piperazineethanesulfonic acid) buffer
[7] DMF: Dimethyformamide

2. Experimental

Journal Pre-proof

2.1. Materials

Para-phenylenediamine (PPDA), 2-hydroxybenzaldehyde (Salicylaldehyde), ammonium thiocyanate (NH_4SCN), bromine (Br_2) and other solvents were obtained from MERCK, Germany, and used as received without further purifications. BSBBT was synthesized for the first time in our lab. Aqueous solutions were prepared using double distilled deionized water.

2.2. Characterization setup

Absorption measurements were acquired from a CARY50, VARIAN Spectrometer, Australia, within the wavelength range of 200–800 nm. Fluorescence measurements were performed on a Varian Cary Eclipse fluorescence spectrophotometer using 1 cm path quartz cell; emission spectra were recorded in the range of 300 to 800 nm. All test solutions were examined using the excitation and emission slit of 5 nm. All spectral investigations were carried out at room temperature. Melting points were recorded by a Stuart SMP3 melting point apparatus. Fourier transform infrared spectra (FT-IR) were obtained from a Tensor 27 spectrophotometer, Germany, using the KBr pellet mode in the region of 4000-400 cm^{-1}. The X-Ray Diffraction (XRD) patterns were collected from a diffractometer, PAN analytical, X' Pert PRO MPD, Netherland, using Ni-filtered Cu Kα radiation (k=1.5418 Å). ^1H NMR (300 MHz) and ^{13}C NMR (75 MHz) spectra were withdrawn from a Bruker Avance DRX-300 spectrophotometer, Germany, with tetramethylsilane (TMS) as the internal standard and $CDCl_3$, DMSO-d_6 and D_2O as the deuterated solvents. Mass spectrum was acquired from a Varian Mat, CH-7 at 70 eV, Mass Spectrometer, Germany. The following abbreviations were used to describe spin multiplicities in ^1H NMR spectra: s = singlet; d = doublet; t = triplet; m = multiplet.

2.3. Spectroscopic measurements

2.3.1. Aggregation induced enhanced emission (AIEE) measurements

Due to insolubility in water, the stock solution of BSBBT (1.0 mM) was prepared from DMSO. The test samples (at fixed concentrations) were prepared by adding 50 µL of stock solution of BSBBT in a 5mL volumetric flask. To furnish 10 µM solution, the samples were diluted by adding the mixtures of

Journal Pre-proof

DMSO/water solution with different water contents, f_w (varies from 0 to 98% v/v). Afterwards, the emission measurements of the resultant solutions were obtained immediately at room temperature.

2.3.2. pH measurements

pH values were measured by 827 pH Lab, Metrohm, Switzerland, equipped with a glass electrode (Thermo Scientific Orion 9157BNMD Triode). pH meter was calibrated with a standard PBS at pH 7.0. The desired pH level was obtained by the addition of 0.1 M NaOH and 0.1 M HCl. The test solutions were prepared by diluting 80 μL of the BSBBT stock solution in 4 mL of PBS. The test solutions were excited at λ_{ex}=268 nm.

2.3.3. Cation sensing measurements

Stock solutions of Al^{3+}, Ba^{2+}, Ca^{2+}, Cd^{2+}, Cr^{2+}, Cu^{2+}, Fe^{3+}, Hg^{2+}, Mg^{2+}, Mn^{2+}, Ni^{2+}, Pb^{2+} and, Zn^{2+} were prepared in deionized double distilled water from their nitrate and chloride salts (10 mM). The test samples were prepared by adding 50 μL of stock solution of BSBBT to 50 μL of stock solutions of metal cations in a 5-mLvolumetric flask. The mixtures were then diluted with PBS at pH=7.4 in order to reach the desired concentration. DL was obtained from the fluorescence titration experiments and calculated from DL=$3\sigma/k$, where, σ is the standard deviation of blank solution (containing BSBBT in the absence of cations) and k is the slope of emission intensity vs. [Pb^{2+}]. Blank measurements were performed ten times using the fluorescence spectrum of blank from which the standard deviation was calculated, while the emission intensity was plotted versus [Pb^{2+}] to find the slope. Parameter K_b (binding constant) was determined from the emission intensity data in the fluorescence titration experiments according to Benesi–Hildebrand equation [44], $1/(I-I_0)=1/(K_b(I_{max}-I_0)[Pb^{2+}])-1/(I_{max}-I_0)$, where I and I_0 represent the emission intensity of BSBBT in the presence and absence of Pb^{2+}, respectively. I_{max} is the saturated emission of BSBBT in the presence of excess amount of Pb^{2+}; $[Pb^{2+}]$ here is the concentration of added Pb^{2+} ion. All test solutions were excited at 276 nm.

2.4. Syntheses

2.4.1. Synthesis of p-Phenylenebis(thiourea) (PBTU)

Journal Pre-proof

PBTU was synthesized according to the procedure introduced in [45] with some changes. To a 250-mL flask, the following items were added: 15.14 g (140 mmol) of PPDA, 126 mL distilled water, 28 mL of concentrated hydrochloric acid, and 0.98 g of activated charcoal. The mixture was warmed up to 50ºC and transferred into another 250-mL flask after filtration. NH_4SCN (47.95 g, 600 mmol) was added and the mixture stirred at a temperature of 90-100ºC for 20-24 h. The yellow, granular product began to precipitate after 2 h reaction. The mixture was allowed to cool down, and then the product was collected by filtration, washed by 80 mL hot water, and finally dried at 100ºC under reduced pressure. ($C_8H_{10}N_4S_2$): light yellow granular solid, yield: 29.6 g (93.43 %); m.p.: 214-219°C. FT-IR spectrum (cm^{-1}, refer to Fig. 1a): 3344, 3267, and 3173 cm^{-1} (NH and NH_2), 3015, 2061, 1617, 1549, 1511, 1478, 1413, 1314, 1222, 1069 cm^{-1} (C=S), 838, 786, 698, 591, 512 cm^{-1}.

2.4.2. Synthesis of 2,6-Diaminobenzo [1,2-d:4,5-d'] bisthiazole (DABBT)

The compound DABBT was synthesized according to the procedure defined in [45] with some changes. To a stirred suspension of 22.6 g (100 mmol) of PBTU in 105.6 mL of dry chloroform, 12.5 mL solution of (6.24 mmol of Br_2) of bromine in 19 mL of chloroform was added such that the pot temperature remained <50ºC. The orange slurry was stirred at room temperature overnight and then refluxed for 24 h. The mixture was allowed to cool down under a slow stream of argon. The granular orange solid was collected by filtration. The crude product was washed with 45 mL of chloroform, dried in air, and stirred with aqueous sodium bisulfite (15.09 g $NaHSO_3$/114 mL water). The yellow solid was collected by filtration, washed with 38 mL of concentrated ammonium hydroxide, and finally washed with 76 mL of water. The crude DABBT was recrystallized twice from 120 mL of glacial acetic acid, and dried to a constant weight at 85ºC under reduced pressure. ($C_8H_6N_4S_2$): pale yellow feathery needles, yield: 12.07 g (53.5 %); m.p.>350ºC. FT-IR spectrum (cm^{-1}, Fig. 1b): 3390, 3270, and 3173 cm^{-1} υ (NH and NH_2), 3052 cm^{-1} υ (Ar-CH), 1637 cm^{-1} υ (C=N), 1539 cm^{-1} υ (C=C), 1436, 1316, 1114, 1068 cm^{-1} (C=S), 858, 616, 504 cm^{-1}.

Journal Pre-proof

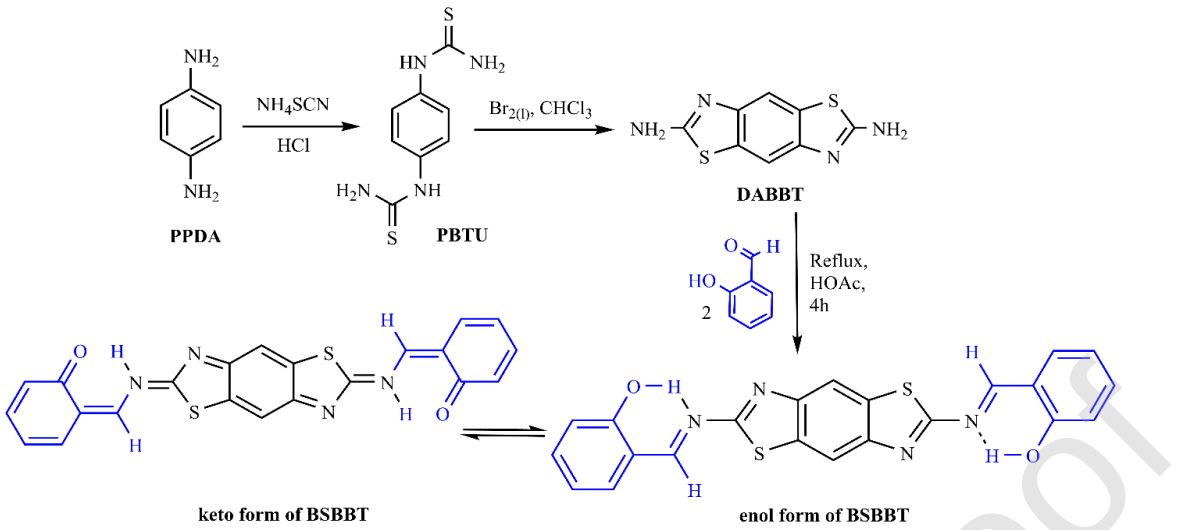

Scheme 1. (Colorful) Synthesis route of BSBBT

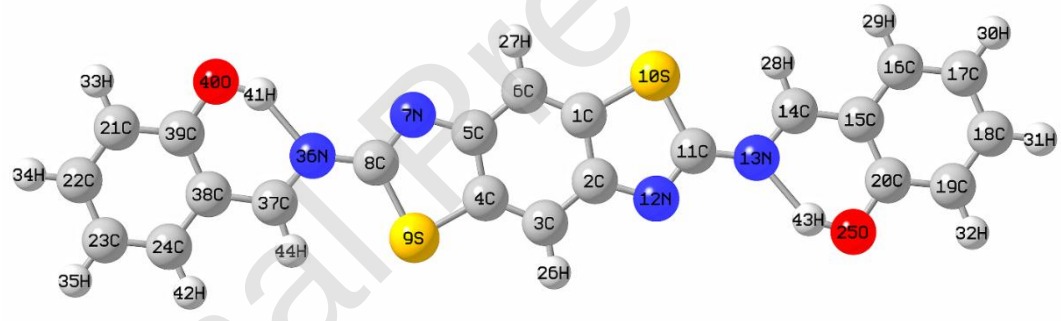

Scheme 2. (Colorful) Optimized spatial view of the enol form of BSBBT using Gaussian 09 software

2.4.3. Synthesis of BSBBT

BSBBT was synthesized in our laboratory for the first time through the following procedure. In a 100 mL flask equipped with a reflux condenser and magnet, Salicylaldehyde (2.61 mL, 25 mmol), DABBT (2.24 g, 10 mmol) and 35 mL glacial acetic acid were mixed and refluxed for 2 h. The hot content of flask was separated from the mixture by using a Büchner funnel, washed with hot ethanol and dried.

Journal Pre-proof

($C_{22}H_{14}N_4O_2S_2$): orange fluorescent solid, yield: 3.4618 g (79.8%); m.p.: 320°C. FT-IR spectrum (cm^{-1}, Fig. 1c): 3442 cm^{-1} (O-H phenol), 1626 cm^{-1} υ (C=N), 1520, 1287, 1174, 761, 572, 451 cm^{-1}. ^1H NMR (300 MHz, DMSO-d_6, TMS); δ (ppm): 10.25, 10.75 (s, 2H, OH), 7.63 (s, 2H, Ar-CH), 7.65-7.70 (dd, 2H, Ar-CH), 7.50-7.60 (td, 4H, Ar-CH), 7.0-7.1 (m, 2H, Ar-CH) (Fig. 2).^{13}C NMR (75 MHz, DMSO-d_6); δ (ppm): 192.19, 165.36, 161.19, 148.16, 136.91, 129.67, 122.76, 119.97, 117.69, 110.08 (Fig. 3).

Journal Pre-proof

Journal Pre-proof

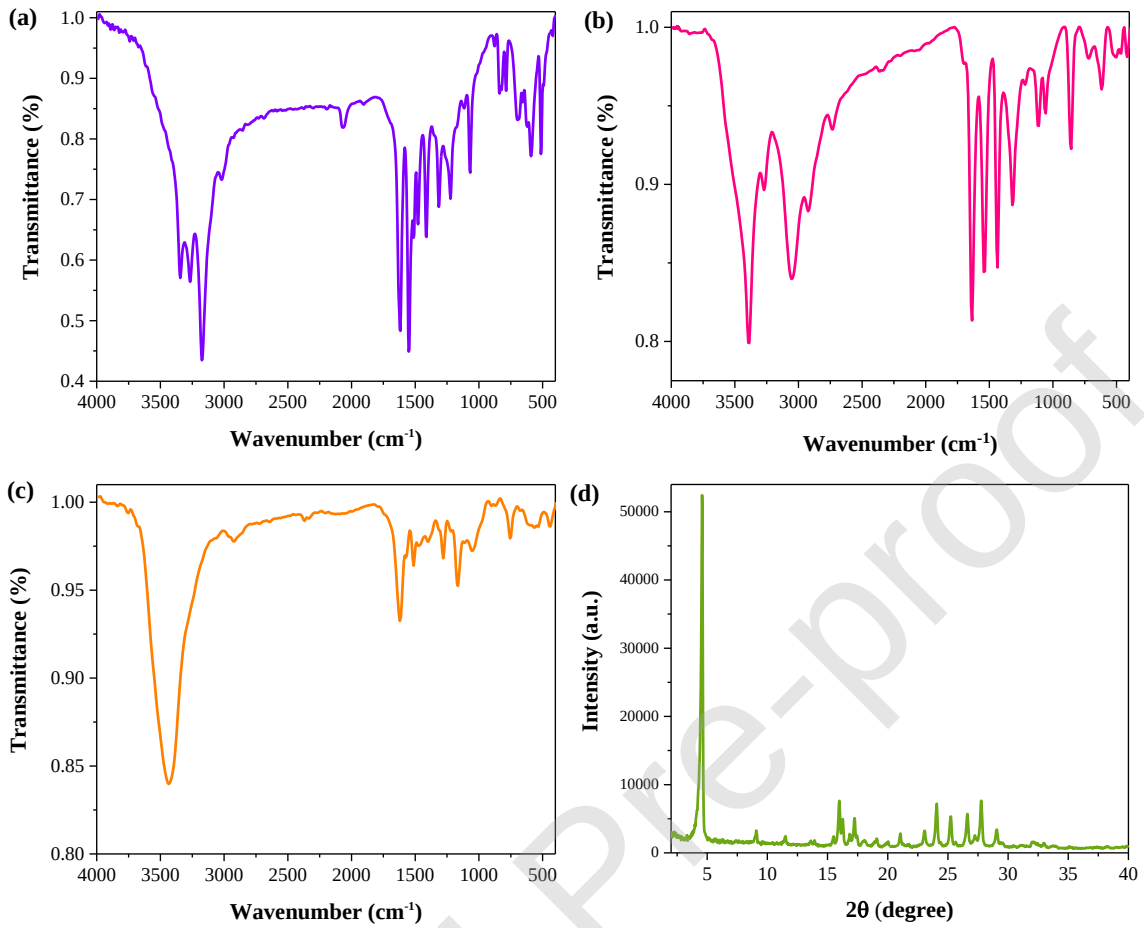

Figure 1. (Colorful) FT-IR spectra of: (a) PBTU, (b) DABBT, (c) BSBBT, and, (d) XRD pattern of BSBBT.

Journal Pre-proof

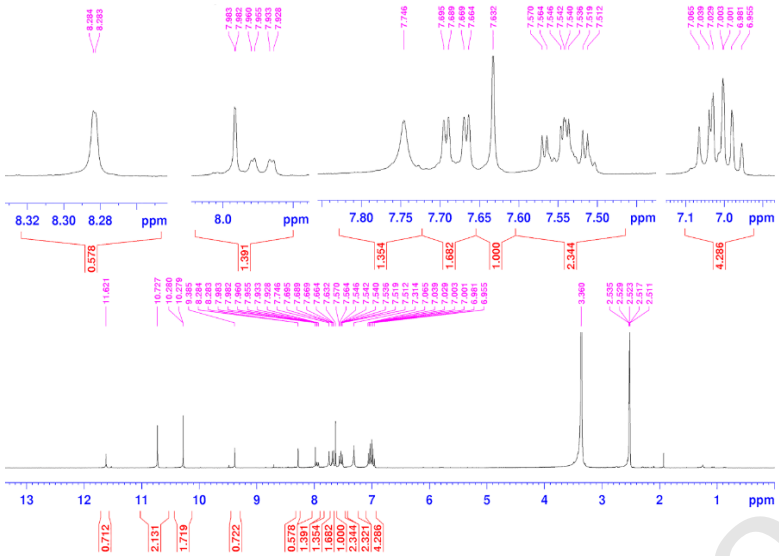

Figure 2. (Colorful) ^{1}H NMR (300 MHz, DMSO-d_6) spectrum of BSBBT

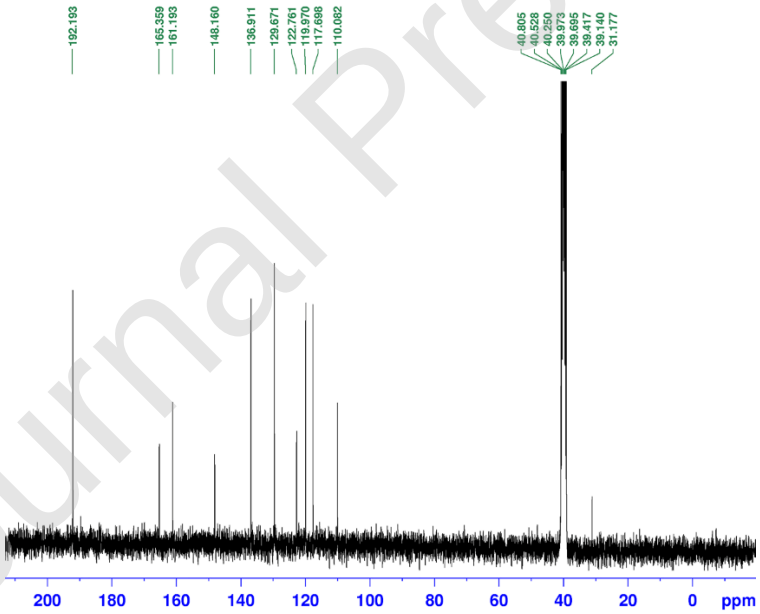

Figure 3. (Colorful) ^{13}C NMR (75 MHz, DMSO-d_6) spectrum of BSBBT

Journal Pre-proof

Journal Pre-proof

3. Results and discussion

A novel luminophore, BSBBT, was facilely synthesized through a simple one-step cost effective Schiff-base condensation reaction between DABBT and salicylaldehyde (1:2 mole ratio) in an acidic medium (Scheme 1); pure orangish precipitate was obtained with an excellent yield. The molecular structure of Schiff-base BSBBT was well-characterized by several techniques, including FT-IR (Fig. 1a-c), XRD patterns (Fig. 1d), ^{1}H NMR (Fig. 2), and ^{13}C NMR (Fig. 3). BBTz chromophore with heteroatoms (Nitrogen and Sulfur) acted as a good chelator for selectively binding heavy and transition metal cations [15]. XRD results of as-prepared BSBBT solid exhibited multiple strong and sharp diffraction peaks, implying that the sample was in a polymorphous microcrystalline state [46].

3.1. UV-Visible absorption and fluorescence emission spectra

Optical characteristics of ligand BSBBT (20 μM) were investigated through the normalized absorption and fluorescence emission spectra both in solutions (DMSO as aprotic solvent, PBS and protic solvent) and in solid state at room temperature; the results were tabulated in Table 2.

Table 2. Optical characteristics of chromophore BSBBT (20 μM) in solution and solid-state.

State	**Color**	**Solvent**	**Absorption** λ_{abs} (nm)	**Fluorescence intensity** (nm)		**Stokes Shift** (nm)
				λ_{ex}	λ_{em}	
Solution	yellow	DMSO	301	276	332 (Broad), 552 (Weak)	31
	yellow-green	PBS	294 (sharp) 378 (broad)	268	538 (Sharp)	160
				276	554 (Sharp)	176
				350	702 (Sharp), (near infrared region (NIR), 700-900)	324
				360	722 (Sharp), (NIR, 700-900)	344
				374	748 (Sharp), (NIR, 700-900)	370
				381	762 (Sharp), (NIR, 700-900)	384
				389	778 (Sharp), (NIR, 700-900)	400
Solid-State	orange	-	-	250	420 (Broad), 460 (Broad)	-
		-	-	370	415 (Broad)	-

BSBBT was not dissolved in some organic solvents such as chloroform, acetone, triethylorthoformate, 1,2-dichloromethane, THF and acetonitrile. However, it was readily dissolved in toluene and ethylacetate

Journal Pre-proof

but non-emissive in these solvents. Further, BSBBT was solved in DMSO and DMF (Lewis-base aprotic solvents) after 15 minutes stirring at 70°C, but it was insoluble in water with strong orange emission in its solid-state (Fig. 4c, and Table 2). As illustrated in Fig. 4a, the observed maximum absorption at 301 nm in DMSO originated from the π-π* intermolecular H-bonding between O-H of salicylaldehyde and imine-N atom of ligand. This rigidified the molecular conformation and led to sharp and intense peaks in buffer solution [47]. To some extent, BSBBT had a fluorescence emission in DMSO because of its enough high viscosity and aprotic properties to slow down the non-radiative intramolecular rotations around C=N linkages available in the salicylidene and BBTz moieties, restricting the intramolecular rotation mechanism in BSBBT through the coplanar association with the process. As a matter of fact, the ESIPT process is the intramolecular proton transfer process between O-H of salicylaldehyde and imine-N atom of ligand, which significantly rigidifies the molecular conformation. So, the large Stokes shift (~160 nm) indicated that when the enol form of BSBBT was rapidly rearranged to the excited keto form, the ESIPT process occurred. This phenomenon was responsible for the strong red-shifted emission at 538 nm in buffer and a weak and broad peak at 300-400 nm in DMSO (Fig. 4b).

For ESIPT properties, the fluorescence characterization of BSBBT probe was examined through several experiments. The fluorescence behavior of BSBBT at varied concentrations in methanol showed slight increase after dilution in methanol. Also, the emission intensity decreased by the increment of excitation wavelength in DMSO (Figs. S1-S4, Table A, Supplementary Information). The pH-dependent behavior of BSBBT was a piece of fact for the existence of different species (both enol- and keto-forms) in the solution. The DFT calculations confirmed the tautomerization process in the excited state through time dependent Self-Consistent Field (TD-SCF) semi-empirical AM1 basis set calculations, where the total energy (E_T) of enol- and keto-forms of BSBBT were characterized as 4.2394 and 8.6503 eV, respectively. As expected, the keto-form of BSBBT was energetically more stable than its enol-form in the first excited singlet state, but in the ground state, the enol-form of BSBBT was energetically more stable than its keto-form (Fig. S5).

Journal Pre-proof

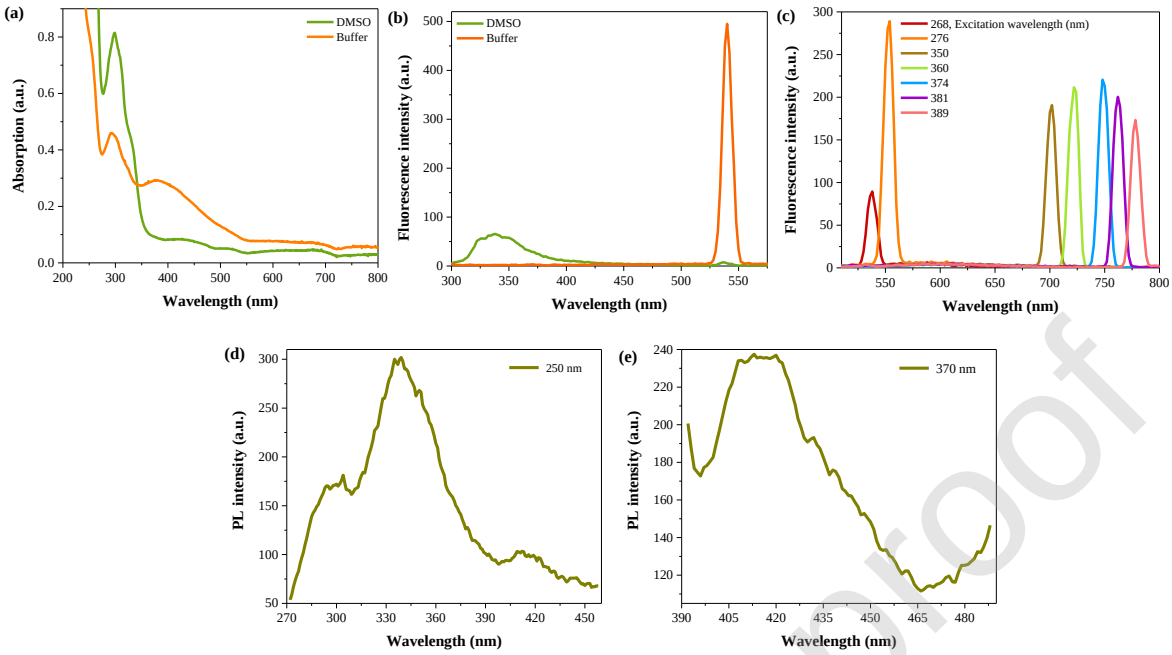

Figure 4. (Colorful) Photo-physical study of BSBBT (20 μM) at room temperature; (a) absorption spectra in DMSO (olive) and PBS (orange), (b) emission spectra in DMSO (olive) and PBS (pH=7.4) (orange), λ_{ex}=268 nm, (c) emission spectra in PBS (pH=7.4) at various excitation wavelengths, (d) solid-state photo-luminescence (PL) spectra, λ_{ex}=250 nm, and, (e) solid-state PL spectra, λ_{ex}=370 nm.

3.2. AIEE behavior of BSBBT

To examine the AIEE activity of BSBBT (10 μM) molecule, we probed the emission behavior in DMSO/water (solvent/non-solvent) binary mixtures. As revealed in Figs. 5a and 5b, BSBBT exhibited a distinct fluorescent behavior in DMSO/H_2O mixture with various water fractions (f_w). Initially, BSBBT showed weak fluorescence in pure DMSO solution; it became stronger at f_w = 40% when the suspension was formed in the DMSO/H_2O mixture. The fluorescence intensity showed a sudden maximum increase at f_w=70%. The solutions emitted bright yellow-green light while the emission intensity of this water content was ~66 times higher than that in pure DMSO solvent, verifying BSBBT as a good AIEE-active compound. The unique fluorescent behavior of BSBBT can be ascribed to the ESIPT property of salicylaldehyde Schiff-base derivatives which are responsible for the narrower and higher intense

Journal Pre-proof

emission peaks. This property reduced the intermolecular interactions in aggregate or in the solid-state, and brought difficulty to the cis-trans isomerization of C=N group [47]. When a large amount of non-solvent (f_w>60%) existed in the mixture BSBBT molecules tended to aggregate [48]. As the aggregation directly affected the molecular arrangement, conformational flexibility, and intermolecular interactions, the novel solid-state properties of fluorophores expected to be correlated to the AIEE phenomenon [48]. PL spectra of BSBBT in Figs. 4d and 4e depict the strong and broad fluorescence emission under 250 and 370 nm excitation wavelengths for the solid-state luminescence of BSBBT [49].

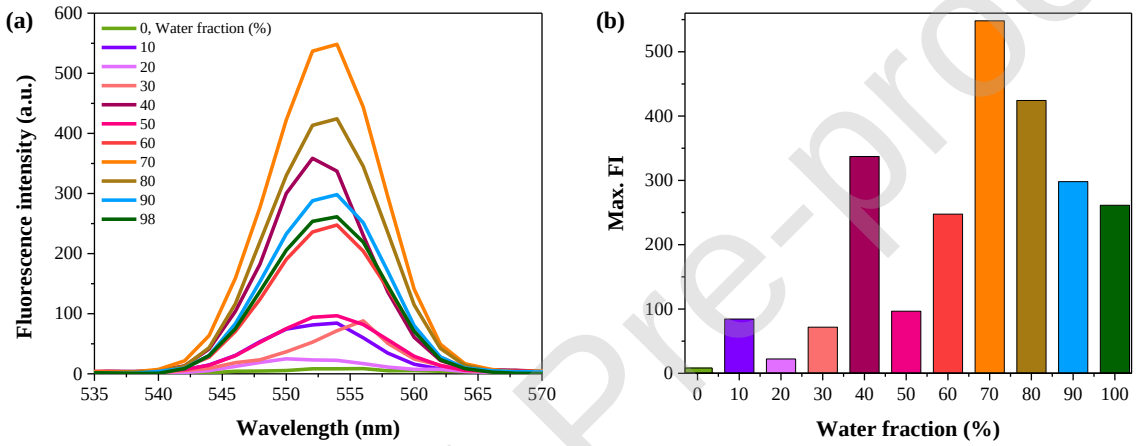

Figure 5. (Colorful) The AIEE behavior of BSBBT (10 μM) in DMSO/H_2O mixture through increasing f_w from 0 to 98%, (v/v), λ_{ex} = 276 nm: (a) emission spectra, and, (b) bar diagram of Maximum Fluorescence Intensity (Max. FI) vs. water fraction.

3.3. pH effect

The pH-dependent behavior of BSBBT was investigated by altering the pH value of aqueous solution within the range of pH=3-11 (Fig. 6). A gradual increase in the fluorescence intensity was observed when the pH increased from 3 to 7; the maximum emission intensity occurred at pH=7 indicating the efficient potential of BSBBT for physiological pH range. After pH=7, the emission intensities at pH 5 and 6 were maximum.

Journal Pre-proof

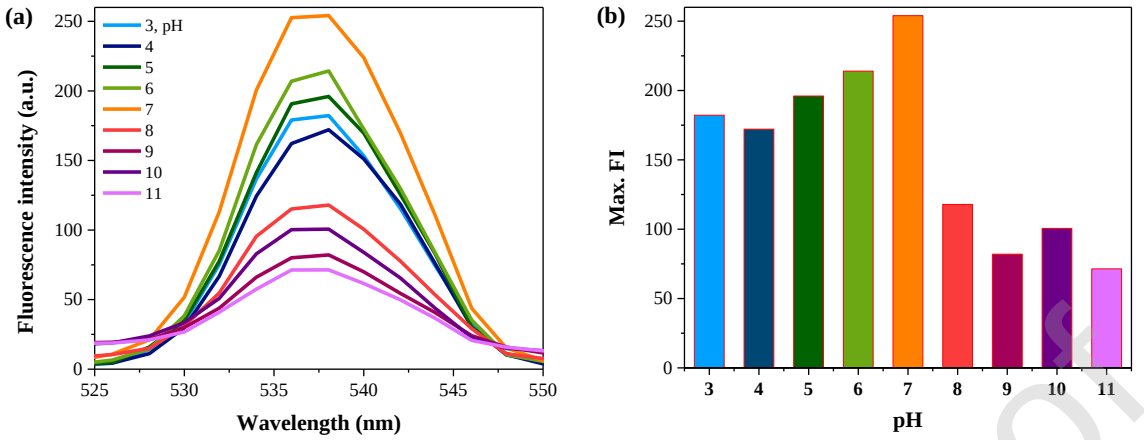

Figure 6. (Colorful) Fluorescent pH-dependent behavior of BSBBT (20 μM) at various pHs in PBS at room temperature; (a) fluorescence spectra, and, (b) Maximum Fluorescence Intensity (Max. FI) vs. pH, λ_{ex} = 268 nm.

3.4. Fluorescence-base cation sensing

For the selectivity, the fluorescence response of BSBBT to various metal cations was investigated. In the absence of metal cations, BSBBT (10 μM) showed very weak emission in PBS (pH=7.4). Fast isomerization around C=N and photo-electron transfer from the nitrogen of benzobisthizole to salicylidene moiety fluorophore were the probable cause of weak fluorescence of BSBBT [50]. Fig. 7a represents the fluorescence emission spectra of BSBBT induced by various metal ions (0.1 m M), including Al^{3+}, Ba^{2+}, Ca^{2+}, Cd^{2+}, Cr^{2+}, Cu^{2+}, Fe^{3+}, Hg^{2+}, Mg^{2+}, Mn^{2+}, Ni^{2+}, Pb^{2+} and Zn^{2+}. Among the examined metal cations, only Pb^{2+} ion significantly enhanced the fluorescence signal with no color change (Fig. 7b). No significant response was seen after adding other metal cations. This fluorescence enhancement was attributed to the inhibition of non-radiative process by the conjugation of Pb^{2+} ions with the C=N linkage available in salicylidene and BBTz moieties [51]. The imine-N was essential for the chelation with most metal ions (Fig. 9); the involvement of imine-N with benzobisthiazole N/S during the chelation with Pb^{2+} ions ceased the isomerization process and increased the fluorescence activity as a result of chelation enhanced fluorescence emission (CHEF) effect [52]. No color change was observed

Journal Pre-proof

with naked eyes. Pb^{2+} ions interacted with both hard and soft binding sites. The BSBBT ligand provided suitable number of proper binding sites, thus, BSBBT displayed a high selectivity for Pb^{2+} ions [53]. To further evaluate the selectivity of BSBBT as an effective fluorescent sensor for Pb^{2+}, a series of competitive experiments were performed on BSBBT in the presence of various metal ions (Fig. 7c); there was no interference by other metal ions. As a result, BSBBT could serve as a selective fluorescent sensor for the recognition of Pb^{2+} ions without any interference of other metal ions.

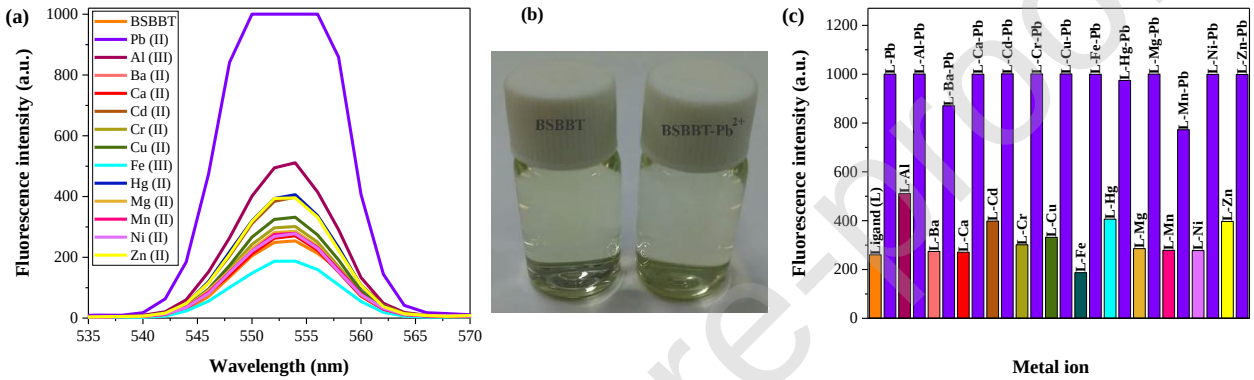

Figure 7. (Colorful) (a) Fluorescence spectral response of BSBBT (10 μM) to various metal cations (0.1 mM), (b) BSBBT solution (left) and BSBBT-Pb^{2+} solution (right), (c) fluorescence intensity of BSBBT against various metal ions with (violet bars) and without (colorful bars) Pb^{2+} in PBS, pH=7.4, λ_{ex} = 276 nm.

Fluorescence titration experiments were performed in order to have further insight into the sensing behavior of BSBBT towards Pb^{2+}. Fig. 8a verified the gradual increase of fluorescence intensity upon the rise in the concentration of Pb^{2+}. The perfect linear relationship of fluorescence intensity vs. [Pb^{2+}] ions is obvious (Fig. 8b). DL was determined as 2.23×10^{-6} M (slope = 28.12573, R^2 = 0.98566). The parameter K_b of BSBBT towards Pb^{2+} was calculated as 0.41×10^{5} M^{-1} (R^2 = 0.95663) (Fig. 8c). These results suggest BSBBT compound as a highly selective and sensitive chemo-sensor for targeting Pb^{2+} in PBS over a wide range of metal ions without any interference from other components.

Journal Pre-proof

In order to determine the binding ratio between BSBBT and Pb^{2+}, the Job's plot experiment was performed (Fig. 8d) where the $A_0/(A-A_0)$ of BSBBT at λ_{Abs}=353.9 nm was plotted against the molar fraction of BSBBT ([BSBBT]/([BSBBT] + [Pb^{2+}])). As a result, the concentration of BSBBT-Pb^{2+} complex approached the maximum at the BSBBT molar fraction of ~0.31, indicating the binding of BSBBT with Pb^{2+} at a binding stoichiometry of 1:2.

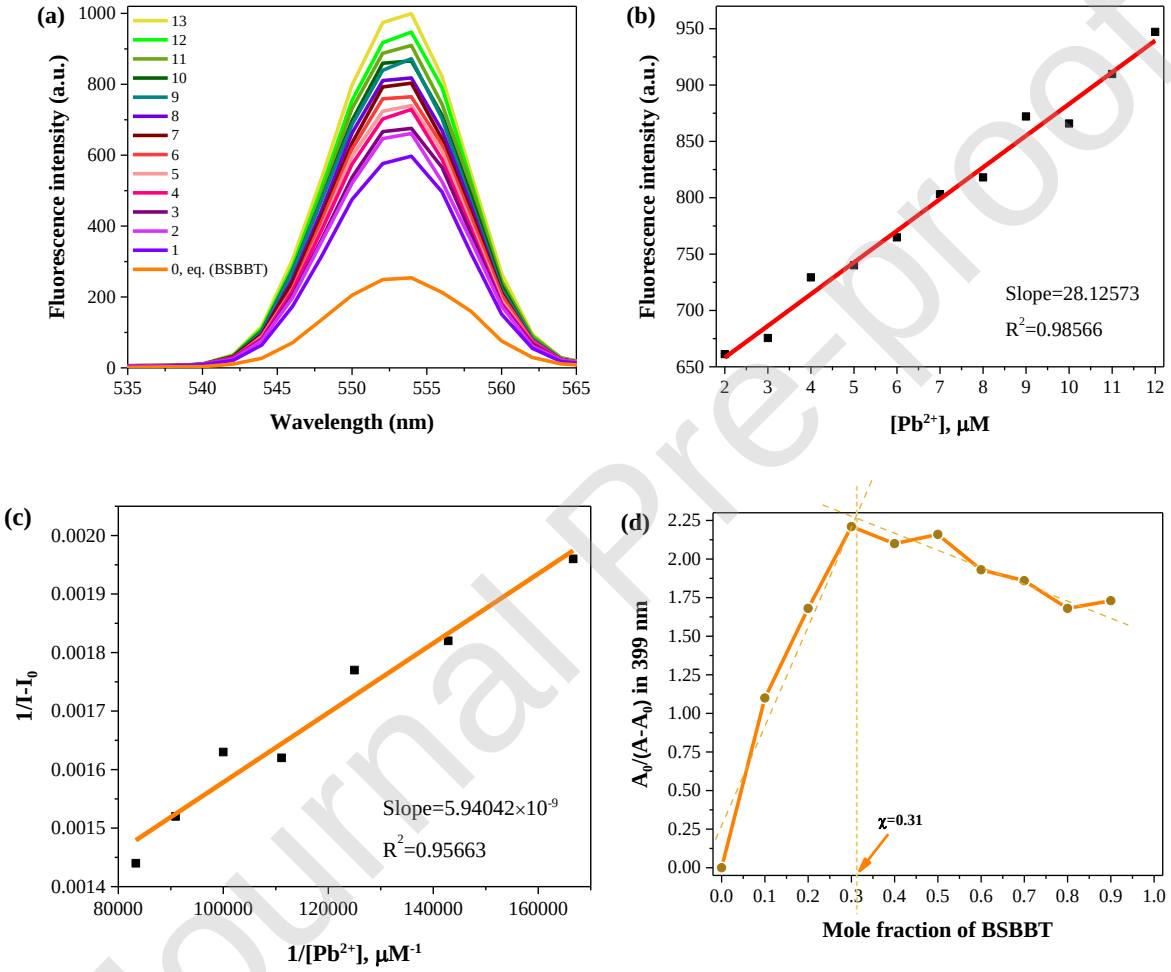

Figure 8. (Colorful) (a) Fluorescence spectra of BSBBT (10 µM) upon the addition of Pb^{2+} at various concentrations (2-12 µM) in PBS, pH=7.4, λ_{ex}=276 nm, (b) fluorescence intensity vs. increasing concentration of Pb^{2+}; calculated DL: 2.23×10^{-6} M, (c) Benesi–Hildebrand plot; calculated K_b: 0.41×10^{5} M^{-1}, and, (d) Job's plot of BSBBT-Pb^{2+} complex, $A_0/(A-A_0)$ vs. molar fraction of BSBBT in the aqueous

Journal Pre-proof

methanolic solution. Job's plot showed the binding stoichiometry of 1:2 for BSBBT/Pb^{2+} at the mole ratio of 0.31.

3.5. DFT Computation

Quantum chemical calculations were carried out to gain further insight into the optical structure, geometry and energy difference between the frontier orbitals of compounds BSBBT and BSBBT-Pb^{2+}; the Highest Occupied Molecular Orbital (HOMO) and the Lowest Unoccupied Molecular Orbital (LUMO). The planar and linear structure and frontier molecular orbitals of BSBBT were explored after optimizing the molecular structure using the Gaussian 09 quantum chemistry packages, DFT/B3LYP/6–31G+(d,p) and DFT/B3LYP/LanL2DZ method for BSBBT and BSBBT-Pb^{2+}, respectively. Visualization of the optimized geometrical structures, frontier molecular orbitals, and electrostatic potential mapped onto the electron density surfaces were performed by GaussView 5. The optimized geometries of BSBBT ligand and BSBBT-Pb^{2+} complex and their corresponded HOMO-LUMO orbitals are presented in Fig. 9. The calculated energy gap (ΔE, eV) of BSBBT and BSBBT-Pb^{2+} were obtained from HOMO and LUMO energy eigen values:

$$\Delta E\ (BSBBT) = E_{LUMO}\text{-}E_{HOMO} = -0.09978 - (-0.21202) = 0.11224\ (eV) \quad (1)$$

$$\Delta E\ (BSBBT\text{-}Pb^{2+}) = E_{LUMO}\text{-}E_{HOMO} = -0.12783 - (-0.10454) = -0.02329\ (eV) \quad (2)$$

Decreased energy gap (ΔE) of BSBBT-Pb^{2+} to -0.02329 (eV) confirmed the significant stability of BSBBT-Pb^{2+} when compared to BSBBT.

Journal Pre-proof

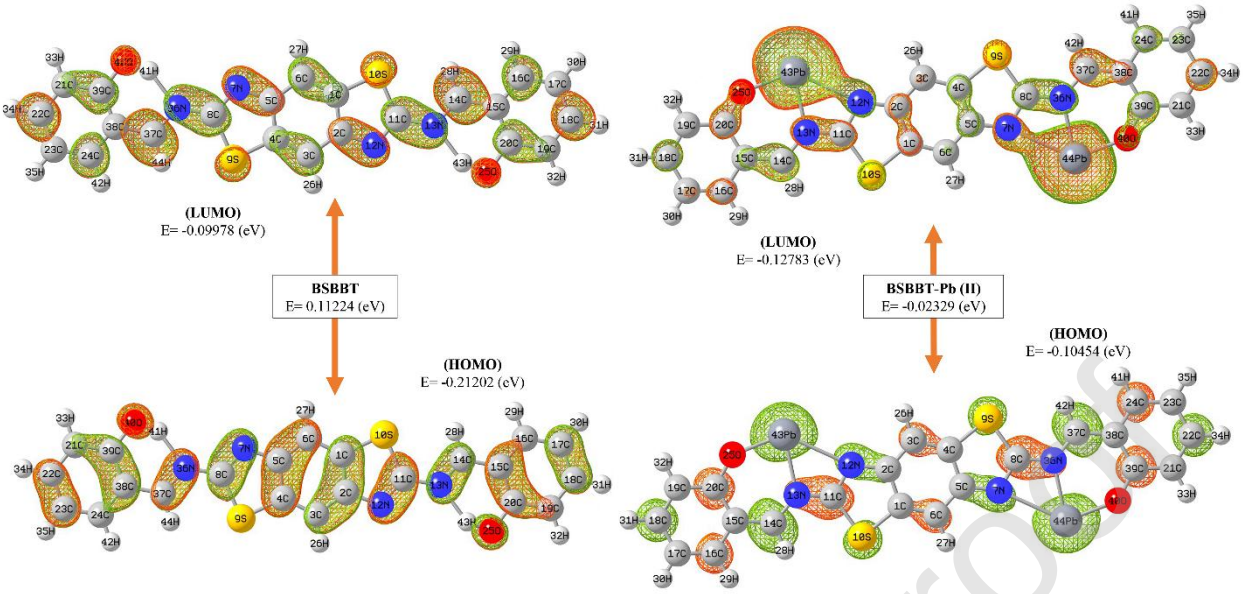

Figure 9. (Colorful) The optimized geometry and HOMO-LUMO energy gap for BSBBT and BSBBT-Pb^{2+} complex using DFT/B3LYP/6–31G+ (d, p) and DFT/B3LYP/ LanL2DZ methods, respectively by Gaussian 09 software.

As a result of complex formation, some of the optimized geometrical parameters of ligand, including bond lengths and bond angles, were changed including the elongation of imine and C=O bond lengths as a result of complexation with Pb^{2+} (Table 3). In addition, Molecular Electrostatic Potential (MEP) mapping was performed to visualize the relative polarity and reactivity of active molecular sites. MEP of BSBBT (Fig. 10a) shows the nucleophilic regions which are electron rich areas located around the electronegative atoms; N and O. The nucleophilic sites in the BSBBT molecule are suitable and susceptible to react with the electron deficient species (electrophilic sites), such as Pb^{2+} ions, in order to tightly create bonded BSBBT-Pb^{2+} complex. This strong interaction pulls the charge of nucleophile towards empty orbitals of Pb^{2+} cation (electrophile) in the sensory process of Pb^{2+} by BSBBT (Fig. 10b) [54].

Journal Pre-proof

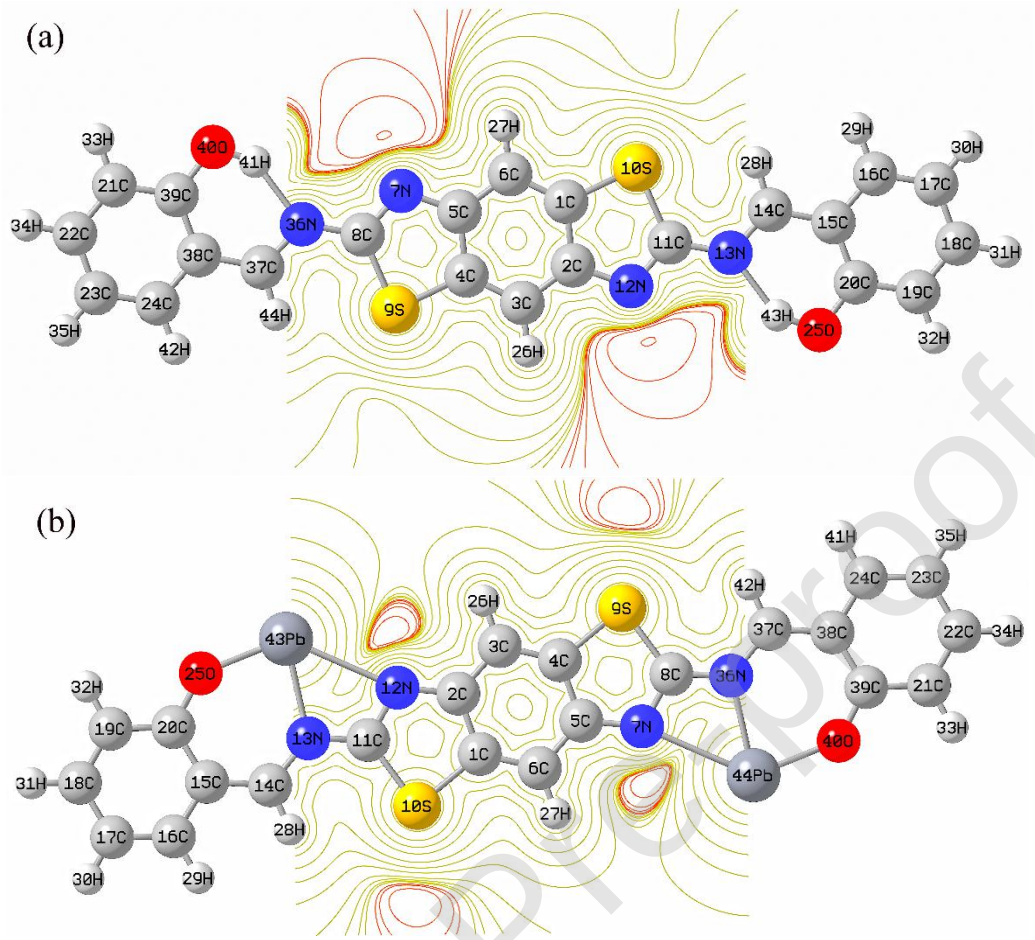

Figure 10. (Colorful) MEP of (a) BSBBT and (b) BSBBT-Pb^{2+} complex obtained from DFT calculations.

Table 3. Bond lengths and bond angles of BSBBT and BSBBT-Pb^{2+} complex obtained from DFT calculations.

Bond length (Å)			**Bond angle (degree)**		
Bond	BSBBT	BSBBT-Pb^{2+}	Bond	BSBBT	BSBBT-Pb^{2+}
C11-N13	1.37110	1.35043	N12-C11-N13	121.66858	117.57768
C14-C15	1.43766	1.42708	C11-N13-C14	122.95927	127.46268
C20-O25	1.33582	1.35955	C11-N13-H43	136.61337	104.14449
O25-Pb43	0.99526	2.07052	S10-C11-N13	123.32050	128.25606
N13-Pb43	1.73744	2.29572	N13-C14-C15	121.82646	125.99197

Journal Pre-proof

4. Conclusion

A novel symmetric tridentate fast-response turn-on fluorescent sensor was introduced and facilely synthesized based on the benzobisthiazole-salicylidene Schiff-base derivative with high yield. The photophysical analysis showed an enhanced emission in the aggregates with excellent AIEE property in both DMSO/H_2O solution and solid state. Tautomerization of keto/enol or hydrogen bonding interactions in the molecule originated the large Stokes shifts and ESIPT properties which introduced it as a useful material for biological photonic devices. BSBBT performed as a highly selective and sensitive benzobisthiazole-based fluorescent sensor for detecting Pb^{2+} ions in PBS at pH=7.4. CHEF effect outreached a good detection limit as low as 2.23×10^{-6} M and strong K_b of 0.41×10^{5} M^{-1} without any interferences from other metal cations co-existed in the solution. DFT calculation for chemo-sensor BSBBT were carried out and confirmed the stability of complex with a lower energy gap (ΔE) of BSBBT-Pb^{2+} complex, supporting the experimental sensing results. By emitting light in the yellow-green region, BSBBT showed an excellent AIEE-activity in DMSO/buffer (30:70, v/v) solution and maximum fluorescence response at pH=7, which qualify it for biological probes. As far as we know, BSBBT is the first multi-responsive benzobisthiazole-base luminescent sensor for the detection of Pb^{2+} ions in PBS at the physiological pH range.

Conflicts of interest

The authors declare no competing financial interest.

Declaration of interests

The authors declare that they have no known competing financial interests or personal relationships that could have appeared to influence the work reported in this paper.

The authors declare the following financial interests/personal relationships which may be considered as potential competing interests:

Acknowledgement

The authors express their gratitude to Islamic Azad University, Mashhad Branch, for the financial support. The Australian College of Kuwait is highly acknowledged for providing the Research Grants No:

Journal Pre-proof

IRC-2018/2019-SOE-ME-PR10 and R11 for this study. Also, special thanks go to Mr. Mohammad Akbar Rahimi and Mrs. Leila Gharaee for their great supports.

Journal Pre-proof

Journal Pre-proof

References

1. Alfonso, M.a., A. Tárraga, and P. Molina, *Ferrocene-based heteroditopic receptors displaying high selectivity toward lead and mercury metal cations through different channels.* The Journal of organic chemistry, 2011. **76**(3): p. 939-947.
2. Madadrang, C.J., et al., *Adsorption behavior of EDTA-graphene oxide for Pb (II) removal.* ACS applied materials & interfaces, 2012. **4**(3): p. 1186-1193.
3. Kim, H.N., et al., *Fluorescent and colorimetric sensors for detection of lead, cadmium, and mercury ions.* Chemical Society Reviews, 2012. **41**(8): p. 3210-3244.
4. Hu, J. and M.S. Elioff, *Detection of Zn2+, Cd2+, Hg2+, and Pb2+ ions through label-free poly-L-glutamic acid.* Talanta, 2018. **188**: p. 552-561.
5. Li, T., S. Dong, and E. Wang, *A lead (II)-driven DNA molecular device for turn-on fluorescence detection of lead (II) ion with high selectivity and sensitivity.* Journal of the American Chemical Society, 2010. **132**(38): p. 13156-13157.
6. Deo, S. and H.A. Godwin, *A selective, ratiometric fluorescent sensor for Pb2+.* Journal of the American Chemical Society, 2000. **122**(1): p. 174-175.
7. Liu, C.-W., C.-C. Huang, and H.-T. Chang, *Highly selective DNA-based sensor for lead (II) and mercury (II) ions.* Analytical chemistry, 2009. **81**(6): p. 2383-2387.
8. Chang, I.-H., et al., *Miniaturized lead sensor based on lead-specific DNAzyme in a nanocapillary interconnected microfluidic device.* Environmental science & technology, 2005. **39**(10): p. 3756-3761.
9. Kim, I.-B., et al., *Sensing of lead ions by a carboxylate-substituted PPE: multivalency effects.* Macromolecules, 2005. **38**(11): p. 4560-4562.
10. Kumar, V.V., T. Raman, and S.P. Anthony, *Fluorescent carbon quantum dots chemosensor for selective turn-on sensing of Zn 2+ and turn-off sensing of Pb 2+ in aqueous medium and zebrafish eggs.* New Journal of Chemistry, 2017. **41**(24): p. 15157-15164.

Journal Pre-proof

11. Kim, S., et al., *Ligand Isomer Effect on the Formations of Supramolecular Lead (II), Mercury (II), and Copper (II)/Mercury (II) Complexes of Bis-O2S2-Macrocycle.* Crystal Growth & Design, 2018. **18**(4): p. 2424-2431.

12. Lin, Y., et al., *Thiazole-based organic semiconductors for organic electronics.* Advanced Materials, 2012. **24**(23): p. 3087-3106.

13. Diaz, E., et al., *Hybrid photoluminescent materials containing a benzobisthiazole core for liquid crystal and gel applications.* Soft matter, 2017. **13**(9): p. 1804-1815.

14. Intemann, J.J., et al., *Synthesis, characterization, and electroluminescence properties of poly (fluorenevinylene benzobisthiazoles).* Journal of Polymer Science Part A: Polymer Chemistry, 2013. **51**(4): p. 916-923.

15. Hrobárik, P., et al., *Quadrupolar benzobisthiazole-cored arylamines as highly efficient two-photon absorbing fluorophores.* Organic letters, 2014. **16**(24): p. 6358-6361.

16. Hrobárik, P., et al., *Benzothiazoles with tunable electron-withdrawing strength and reverse polarity: a route to triphenylamine-based chromophores with enhanced two-photon absorption.* The Journal of organic chemistry, 2011. **76**(21): p. 8726-8736.

17. Hrobárik, P., et al., *Molecular engineering of benzothiazolium salts with large quadratic hyperpolarizabilities: can auxiliary electron-withdrawing groups enhance nonlinear optical responses?* The Journal of Physical Chemistry C, 2010. **114**(50): p. 22289-22302.

18. Papucci, C., et al., *Green/Yellow-Emitting Conjugated Heterocyclic Fluorophores for Luminescent Solar Concentrators.* European Journal of Organic Chemistry, 2018. **2018**(20-21): p. 2657-2666.

19. Mishra, J., N. Kaur, and A.K. Ganguli, *Selective and sensitive fluorescence recognition of Pb (II) in aqueous medium by organic nanoparticles of a urea linker based tetrapodal receptor: Effect of linker molecules in a sensor on chemosensing.* Inorganica Chimica Acta, 2019. **487**: p. 214-220.

Journal Pre-proof

20. Xu, Y., et al., *Switchable and selective detection of Zn 2+ or Cd 2+ in living cells based on 3'-O-substituted arrangement of benzoxazole-derived fluorescent probes.* Chemical Communications, 2014. **50**(56): p. 7514-7516.

21. Serdiuk, I.E., *White light from a single fluorophore: a strategy utilizing excited-state intramolecular proton-transfer phenomenon and its verification.* The Journal of Physical Chemistry C, 2017. **121**(9): p. 5277-5286.

22. Xu, D., et al., *A benzothizole-based fluorescent probe for Hg2+ recognition utilizing ESIPT coupled AIE characteristics.* Tetrahedron Letters, 2017. **58**(37): p. 3654-3657.

23. Gu, B., et al., *A benzothiazole-based fluorescent probe for distinguishing and bioimaging of Hg2+ and Cu2+*. Analytica chimica acta, 2017. **954**: p. 97-104.

24. Chen, S., et al., *2-Hydroxy benzothiazole modified rhodol: aggregation-induced emission and dual-channel fluorescence sensing of Hg2+ and Ag+ ions.* Sensors and Actuators B: Chemical, 2018. **255**: p. 2086-2094.

25. Zhang, H., et al., *A multifunctional tripodal fluorescent probe for the recognition of Cr3+, Al3+, Zn2+ and F− with controllable ESIPT processes.* Dyes and Pigments, 2019. **162**: p. 257-265.

26. Jie, X., et al., *A new colorimetric, near-infrared fluorescent probe for rapid detection of palladium with high sensitivity and selectivity*. Talanta, 2018. **183**: p. 164-171.

27. Chen, Y., et al., *A benzothiazole-based fluorescent probe for ratiometric detection of Al3+ in aqueous medium and living cells.* Industrial & Engineering Chemistry Research, 2017. **56**(43): p. 12267-12275.

28. Lu, Z.-N., et al., *A selective fluorescent chemosensor for Cd2+ based on 8-hydroxylquinoline-benzothiazole conjugate and imaging application.* Spectrochimica Acta Part A: Molecular and Biomolecular Spectroscopy, 2019. **213**: p. 57-63.

29. Zhao, Y.-H., et al., *A novel ratiometric and reversible fluorescence probe with a large Stokes shift for Cu2+ based on a new clamp-on unit.* Analytica Chimica Acta, 2019.

Journal Pre-proof

30. Yu, Y., et al., *A novel benzothiazole-based fluorescent probe for cysteine detection and its application on test paper and in living cells.* Talanta, 2018. **176**: p. 151-155.

31. Li, J., et al., *A benzothiazole-based fluorescent probe for efficient detection and discrimination of Zn2+ and Cd2+, using cysteine as an auxiliary reagent.* Sensors and Actuators B: Chemical, 2018. **268**: p. 446-455.

32. Chang, C., et al., *Benzothiazole-based fluorescent sensor for ratiometric detection of Zn (II) ions and secondary sensing PPi and its applications for biological imaging and PPase catalysis assays.* Industrial & Engineering Chemistry Research, 2017. **56**(31): p. 8797-8805.

33. Tang, Y., et al., *Synthesis of a new pyrene-devived fluorescent probe for the detection of Zn2+.* Tetrahedron Letters, 2018. **59**(44): p. 3916-3922.

34. Gong, J., et al., *A thiazolo [4, 5-b] pyridine-based fluorescent probe for detection of zinc ions and application for in vitro and in vivo bioimaging.* Talanta, 2018. **185**: p. 396-404.

35. Venkatesan, V., S.A. Kumar, and S.K. Sahoo, *Highly selective turn-on fluorogenic chemosensor for Zn2+ based on chelation enhanced fluorescence.* Inorganic Chemistry Communications, 2019. **102**: p. 171-179.

36. Sahana, S., et al., *2-(2'-Hydroxyphenyl)-benzothiazole (HBT)-terpyridine conjugate: A highly specific ICT based fluorescent probe for Zn2+ ions and its application in confocal cell imaging.* Journal of Photochemistry and Photobiology A: Chemistry, 2018. **351**: p. 231-239.

37. Kaur, I., et al., *Excitation wavelength based reversible multicolour photoluminescence by a single chromophore upon aggregation: Detection of picric acid-application in bioimaging.* Sensors and Actuators B: Chemical, 2019. **281**: p. 613-622.

38. Wang, W., et al., *Strategically modified highly selective mitochondria-targeted two-photon fluorescent probe for Au3+ employing Schiff-base: Inhibited C= N isomerization vs. hydrolysis mechanism.* Dyes and Pigments, 2018. **150**: p. 241-251.

39. Wu, X., et al., *Highly Sensitive Ratiometric Fluorescent Paper Sensors for the Detection of Fluoride Ions.* ACS Omega, 2019. **4**(3): p. 4918-4926.

Journal Pre-proof

40. Kaur, I., P. Kaur, and K. Singh, *2-(4-Amino-2-hydroxyphenyl) benzothiazole based Schiff-base: Complexation/decomplexation driven photo physical tuning of fluorescence leading to Cu2+ and PO43− detection.* Sensors and Actuators B: Chemical, 2018. **257**: p. 1083-1092.

41. Wang, H., et al., *A facile fluorescent probe with a large Stokes shift for sequentially detecting copper and sulfide in 100% aqueous solution and imaging them in living cells.* Sensors and Actuators B: Chemical, 2018. **256**: p. 600-608.

42. Xu, W., et al., *A highly selective turn-on fluorescent and chromogenic probe for CN− and its applications in imaging of living cells and zebrafish in vivo.* Sensors and Actuators B: Chemical, 2017. **251**: p. 366-373.

43. Chen, W., et al., *A phenothiazine coumarin-based red emitting fluorescent probe for nanomolar detection of thiophenol with a large Stokes shift.* Sensors and Actuators B: Chemical, 2017. **245**: p. 702-710.

44. Singh, R. and G. Das, *"Turn-on" Pb 2+ sensing and rapid detection of biothiols in aqueous medium and real samples.* Analyst, 2019. **144**(2): p. 567-572.

45. Wolfe, J.F., B.H. Loo, and F. Arnold, *Rigid-rod polymers. 2. Synthesis and thermal properties of para-aromatic polymers with 2, 6-benzobisthiazole units in the main chain.* Macromolecules, 1981. **14**(4): p. 915-920.

46. Shen, X.Y., et al., *Effects of substitution with donor–acceptor groups on the properties of tetraphenylethene trimer: aggregation-induced emission, solvatochromism, and mechanochromism.* The Journal of Physical Chemistry C, 2013. **117**(14): p. 7334-7347.

47. Xu, S., et al., *An organic molecule with asymmetric structure exhibiting aggregation-induced emission, delayed fluorescence, and mechanoluminescence.* Angewandte Chemie International Edition, 2015. **54**(3): p. 874-878.

48. Liu, D., et al., *Rh-Catalyzed C–H Amidation of 2-Arylbenzo [d] thiazoles: An Approach to Single Organic Molecule White Light Emitters in the Solid State.* Organic letters, 2019.

Journal Pre-proof

49. Zhu, H., et al., *Branched triphenylamine luminophores: Aggregation-induced fluorescence emission, and tunable near-infrared solid-state fluorescence characteristics via external mechanical stimuli.* Dyes and Pigments, 2018. **151**: p. 140-148.

50. Gogoi, A. and G. Das, *NIR sensing of Zn (II) and subsequent dihydrogen phosphate detection by a benzothiazole functionalized ninhydrin based receptor.* RSC Advances, 2014. **4**(99): p. 55689-55695.

51. Pu, S., et al., *Multi-addressable molecular switches based on a new diarylethene salicylal Schiff base derivative.* Journal of Materials Chemistry C, 2013. **1**(31): p. 4726-4739.

52. Sedgwick, A.C., et al., *Excited-state intramolecular proton-transfer (ESIPT) based fluorescence sensors and imaging agents.* Chemical Society Reviews, 2018. **47**(23): p. 8842-8880.

53. Wang, L., et al., *Meso-Substituent-Directed Aggregation Behavior and Water Solubility: Directly Functionalizing of Methine Chain in Thiazole Orange and Biological Applications in Aqueous Buffer.* The Journal of organic chemistry, 2019.

54. Walsh, S., A.H. El-Sagheer, and T. Brown, *Fluorogenic thiazole orange TOTFO probes stabilise parallel DNA triplexes at pH 7 and above.* Chemical science, 2018. **9**(39): p. 7681-7687.

Journal Pre-proof